Supporting Information

Hydrophobic species-enabled acid-base multi-catalysis for stereoselective access to renewable trans-anethole

Yixuan Liu, Mingrui Li, Tengyu Liu, Jinyu Tan, Samuel Lalthazuala Rokhum, Heng Zhang*, Song Yang*, Hu Li*

** Corresponding authors.*

Catalyst characterization

Fourier transform infrared (FT-IR) spectra were obtained by PerkinElmer 1710, and the catalyst surface acid type and content were investigated by pyridine-adsorbed FT-IR. Powder X-ray diffraction (XRD) patterns were achieved utilizing a Bruker D8 Advance X-ray analyzer with Cu-Kα (λ = 1.542 Å) radiation and 2θ (5°-90°). Surface area (S_{BET}), pore volume (V_{pore}), and average pore size ($D_{mean)}$ of the catalysts were investigated by N_2 adsorption-desorption on a Micromeritics ASAP 2460 apparatus. Thermogravimetric (TG) and differential scanning calorimetry (DSC) analyses were conducted using NETZSCH STA 449 F3. The catalyst morphology was mainly observed by different electron microscopes, including scanning electron microscope (SEM, ZEISS SIGMA300), high-resolution transmission electron microscope (HR-TEM, JEM-1200EX]), STEM-mapping images (FEI TALOS F200C), and atomic force microscope (AFM, Bruker Innova IRIS). Inductively coupled plasma-optical emission spectrometer (ICP-OES) was recorded on a PerkinElmer Optima 5300 DV to detect the chemical element. ^{31}P MAS NMR spectra were characterized on a Bruker AVANCE III 400 WB, at an 8 kHz spinning rate. The content of S was measured with an elemental analysis (Vario EL Cube, Germany) Contact angles were measured with a Data physics OCA20. CO_2- and NH_3-temperature-programmed desorption (TPD) profiles were obtained by the Micromeritics AutoChem 2920 chemisorption analyzer. X-ray photoelectron spectroscopy (XPS) measurements were carried out using a K-alpha system.

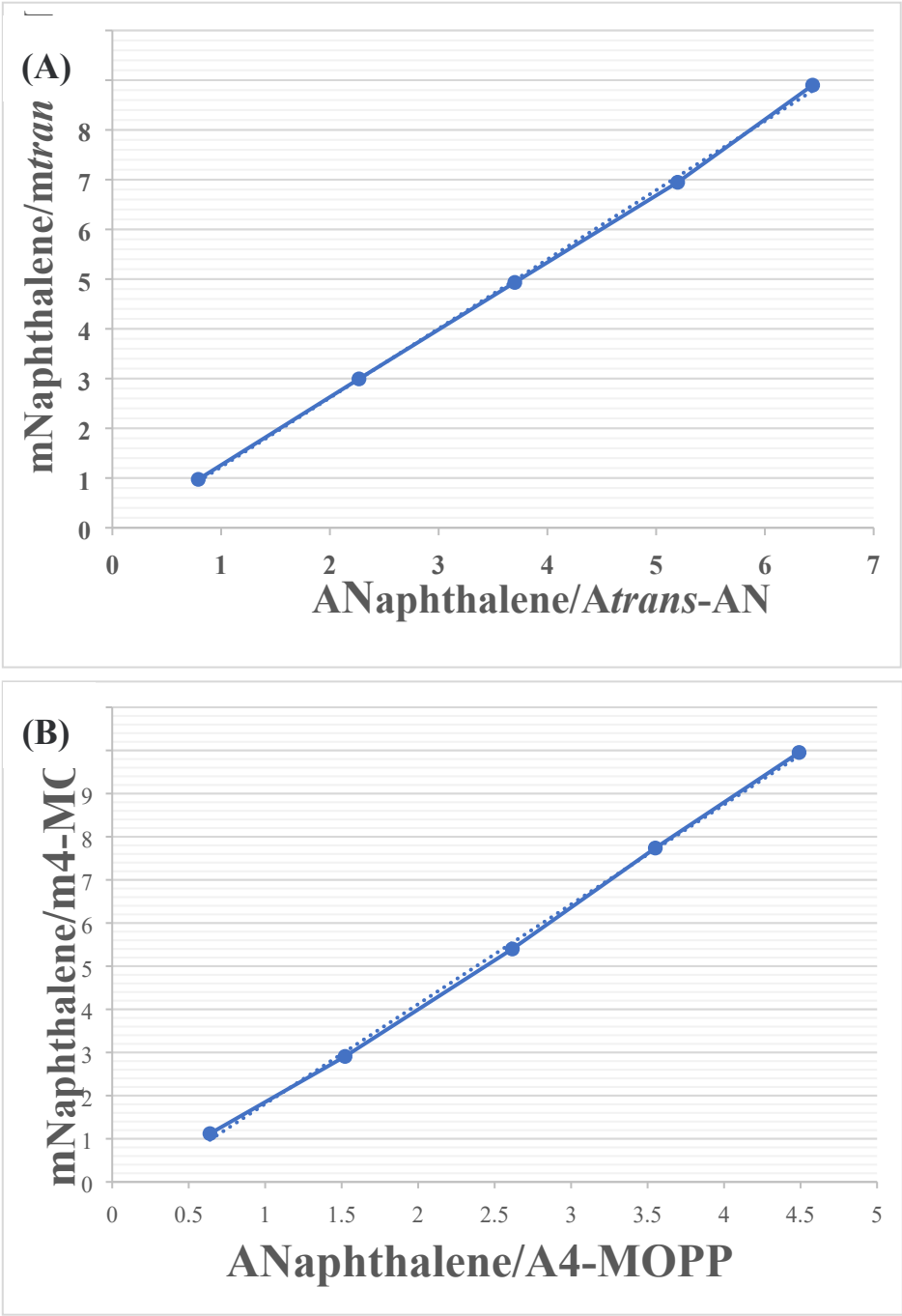

Fig. S1 Internal standard curves for *trans*-AN (A) and 4-MOPP (B).

Table S1 Center composition design matrix together with the experimental response values.

Run	A/°C	B/h	C/mol%	AN Yield/%
1	1	240	13.0	91.1
2	1	200	13.0	63.1
3	2	220	13.0	97.8
4	3	220	19.5	88.6
5	2	220	13.0	98
6	3	220	6.5	78.3
7	3	240	13.0	80.5
8	2	200	19.5	87.1
9	2	220	13.0	94.9
10	2	220	13.0	98.2
11	1	220	19.5	88.3
12	2	240	6.5	90.2
13	3	200	13.0	73.4
14	2	200	6.5	45.6
15	2	240	19.5	91
16	1	220	6.5	72.5
17	2	220	13.0	94.6

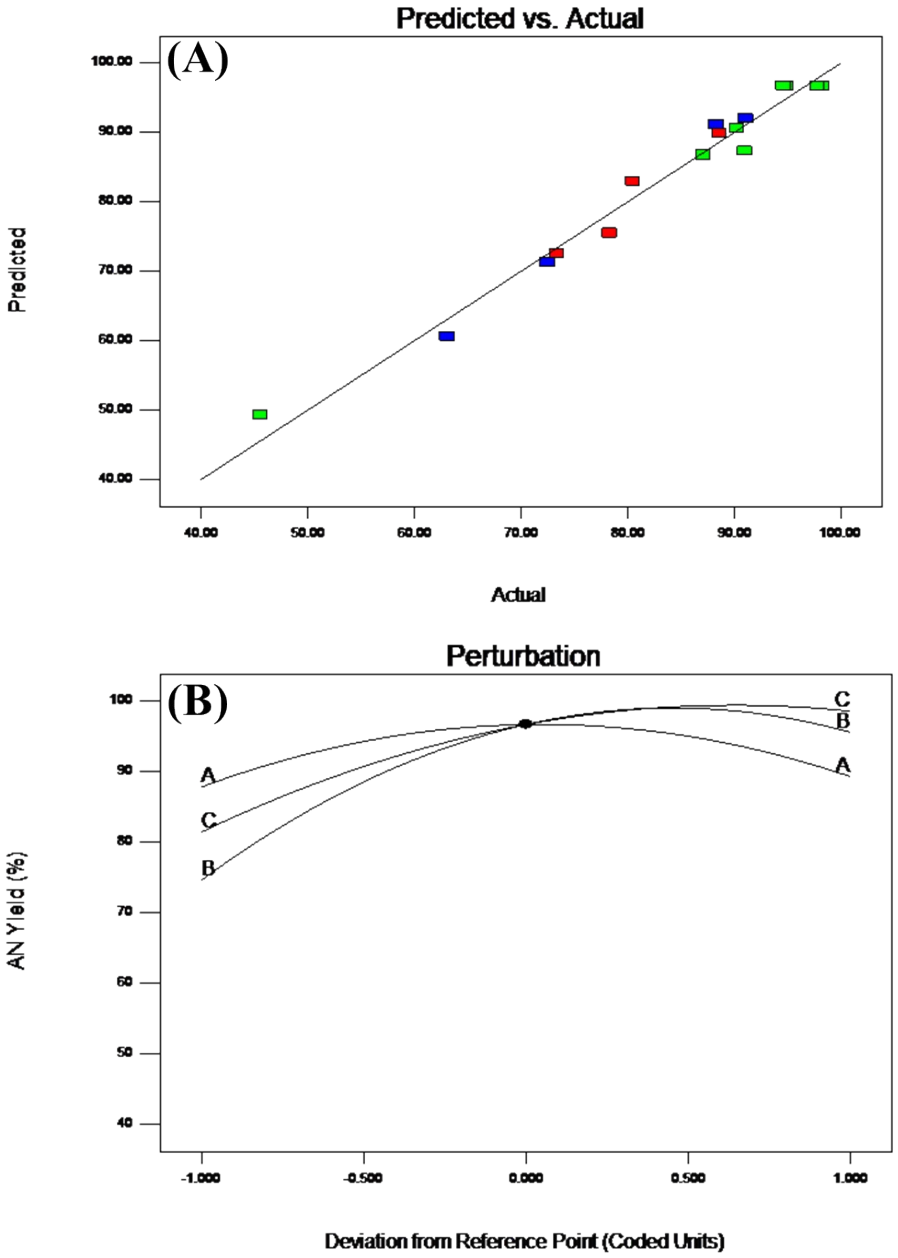

Fig. S2 Parity plot between actual and model predicted of AN yield (A), and perturbation slope of all factors (B)